arXiv:physics/0408102v1 [physics.class-ph] 23 Aug 2004

Ferromagnetic/superconducting bilayer structure: A model system for spin diffusion length estimation

S. Soltan [a,b] , J. Albrecht[a], and H.–U. Habermeier[a]
[a] *Max–Planck–Institut für Festkörperforschung, Heisenbergstr. 1, D–70569 Stuttgart, Germany*
[b] *1.Physikalisches Institut, Universität Stuttgart, Pfaffenwaldring 57, D–70550 Stuttgart, Germany*
(March 31, 2022)

We report detailed studies on ferromagnet–superconductor bilayer structures. Epitaxial bilayer structures of half metal–colossal magnetoresistive $La_{2/3}Ca_{1/3}MnO_3$ (HM–CMR) and high–T_c superconducting $YBa_2Cu_3O_{7-\delta}$(HTSC) are grown on $SrTiO_3$ (100) single–crystalline substrates using pulsed laser deposition. Magnetization M(T) measurements show the coexistence of ferromagnetism and superconductivity in these structures at low temperatures. Using the HM–CMR layer as an electrode for spin polarized electrons, we discuss the role of spin polarized self injection into the HTSC layer. The experimental results are in good agreement with a presented theoretical estimation, where the spin diffusion length ξ_{FM} is found to be in the range of $\xi_{FM} \approx 10$ nm.

I. INTRODUCTION

The antagonism between ferromagnetism and superconductivity has been described very early by Ginzburg[1]. Based on the inverse of the Meissner effect, surface currents shield the external region from being frozen in a magnetic field. Pioneering experiments on classical FM/SC tunneling junctions were carried out by Tedrow and Meservey[2]. In their experiment a ferromagnetic (FM) electrode is used to inject spin–polarized quasiparticles (SPQP) into superconducting layers. The injection of quasiparticles into superconductors creates a local nonequilibrium state which suppresses the superconducting order parameter and the critical current density j_c[3].

Theoretical works on bilayers of metallic ferromagnets and low-temperature superconductors[4,5] predicted oscillations of the critical temperature T_c. This was confirmed by experimental results[6,7]. The oscillating behavior of the superconducting temperature is due to tunneling of Cooper–pairs into the FM layer[8]. A review on this topic is given by Izyumov et al.[9].

In the past few years, much attention has been paid to junctions consisting of $La_{2/3}Ca_{1/3}MnO_3$ (LCMO), a material that shows a colossal magnetoresistance (CMR) effect, and of $YBa_2Cu_3O_{7-\delta}$ (YBCO), a high-T_c superconductor[10–17].

Experiments with these junctions allow to obtain information about the spin–dependent properties of high-T_c superconductors that can lead to the design of new superconducting devices such as "spintronic devices", like transistors with high gain current and high speed. "Spintronics" means the exploitation of the spins of the electrons rather than their charge. Spin controlled solid state devices based on the giant magnetoresistance (GMR) effect are already realized in read-out heads of hard disks. Further challenges in the field of spintronics that are addressed by experiments and theory include the optimization of electron–spin life times and the detection of the spin coherence length in nanoscale structures.

The high spin polarization, in addition to ferromagnetic ordering, is characteristic for hole–doped rare earth manganites of the form $R_{1-x}A_xMnO_3$ (R: trivalent rare–earth ions, A: divalent alkaline–earth ions). In this case the spin polarization of the transport electrons is close to 100 %[18–20].

The fact that the in–plane lattice parameters of $La_{2/3}Ca_{1/3}MnO_3$ and $YBa_2Cu_3O_{7-\delta}$ are very similar allows an epitaxial growth of LCMO/YBCO bilayers with structurally sharp interfaces. These bilayers represent adequate model systems to investigate spin diffusion into high-temperature superconducting films which is shown in this paper.

Recently, several experimental and theoretical efforts have been performed[12,21,22] to determine the spin diffusion length ξ_{FM} in CMR/HTSC multilayered structures, but up to now no clear answer could be given. We show, that in bilayer or superlattice structures of manganites and cuprates the spin diffusion length can be determined from the experimentally observed properties.

We present a rough theoretical estimation for the spin diffusion length in heterostructures of cuprates and manganites. This estimation is able to describe properly the experimental results of bilayer structures and superlattices of CMR/HTSC.

Our results are obtained by investigating epitaxial bilayer structures of thin films of ferromagnetic LCMO and high-T_c superconducting YBCO. A sketch of these samples is shown in Fig. (1). The temperature-dependent magnetization of these samples after zero-field cooling to T = 5 K has been determined to show if a coexistence of ferromagnetism and superconductivity at low temperatures occurs. In these experiments it is found that the superconducting transition temperature of the YBCO film decreases strongly for thicknesses of the superconductor of $d_s = 30$ nm and below. This is in contrast to YBCO single layers, where a thickness dependence of T_c occurs only for films with thicknesses of well below 10 nm[23,24]. The drop of the transition temperature for LCMO/YBCO bilayers can now be described by applying a rough theoretical estimation taking into account the diffusion of spin–polarized quasiparticles with a penetration depth of the order of 10 nm.

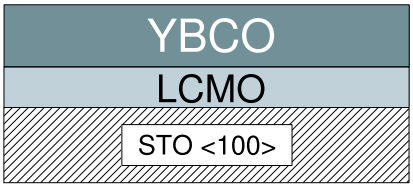


FIG. 1. Sketch of the chosen sample geometry. The $La_{2/3}Ca_{1/3}MnO_3$ (LCMO) and $YBa_2Cu_3O_{7-\delta}$ (YBCO) are grown by pulsed laser deposition onto $SrTiO_3$ (100) single crystalline substrates.

II. EXPERIMENTAL DETAILS

Epitaxial bilayers of $La_{2/3}Ca_{1/3}MnO_3$ and optimally doped $YBa_2Cu_3O_{7-\delta}$ are grown by pulsed laser deposition. The target used for the ferromagnetic layer, that is first deposited, has a nominal composition of $La_{2/3}Ca_{1/3}MnO_3$, the superconducting layer on top is grown by using a target $YBa_2Cu_3O_{6.95}$. As substrates 5×5 mm^2 $SrTiO_3$ (STO) (100) single crystals are used. The substrate is kept at a constant temperature of 780 °C, the temperature is adjusted by a far-infrared pyrometric temperature control. During the deposition an oxygen pressure of 0.4 mbar in case of the LCMO layer and 0.6 mbar during the YBCO deposition is used. Afterwards the bilayer is annealed in-situ for 30–60 minutes at 530 °C in an oxygen pressure of 1.0 bar. This procedure results in films of high crystalline quality, full oxygenation, and sharp film–substrate interfaces[10]. Structural studies are carried out by x-ray diffraction (XRD) at room temperature, the resistance $R(T)$ is measured with evaporated chromium gold contacts using the standard four-probe technique. The temperature dependence of the magnetization M(T) is recorded in a magnetic field parallel to the film plane using a Quantum Design MPMS superconducting quantum interference device (SQUID) magnetometer.

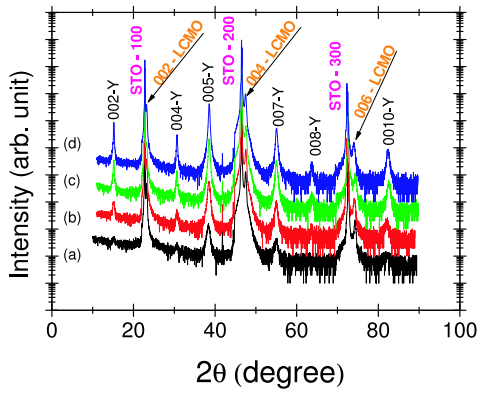


FIG. 2. (Color online) X-ray pattern for the bilayer structures with thicknesses of d_{LCMO} = 50 nm and d_{YBCO}= 20 nm (a), 30 nm (b), 50 nm (c), and 100 nm (d) respectively. Only the (00ℓ) peak is found, i.e. the both layers show c–axis textured growth on the STO (100) substrate.

III. RESULTS AND DISCUSSION

A. X-ray diffraction pattern (XRD)

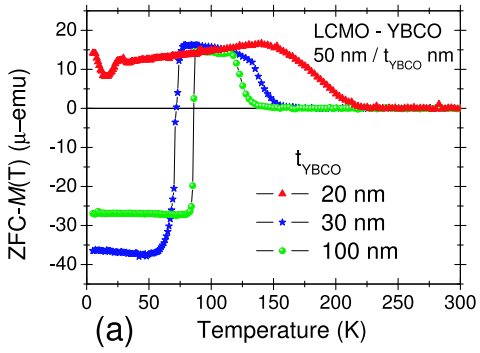
The STO substrate has a perfect cubic perovskite structure and both the magnetic $La_{2/3}Ca_{1/3}MnO_3$ layer and the superconducting $YBa_2Cu_3O_{7-\delta}$ layer have an orthorhombic lattice structure. The important structural information of all of the used materials is given in table (I). The epitaxial YBCO thin film on top of the LCMO layer grows under tensile strain of $\varepsilon \approx 0.4$ %, where ε can be written as: $\varepsilon = [(a_{LCMO} \times b_{LCMO})^{1/2} - (a_{YBCO} \times b_{YBCO})^{1/2}]/(a_{YBCO} \times b_{YBCO})^{1/2}$.

TABLE I. The crystal structure data-base for the all used materials $SrTiO_3$, $La_{2/3}Ca_{1/3}MnO_3$, and $YBa_2Cu_3O_7$.

Material	Lattice Parameter (Å)			Structure	Space group
	a	b	c		
$SrTiO_3$	3.905			cubic	$Pm\bar{3}m$(221)
$La_{2/3}Ca_{1/3}MnO_3$	3.868	3.858	5.453	orthorhombic	Pbnm(62)
$YBa_2Cu_3O_7$	3.817	3.883	11.682	orthorhombic	Pmmm(47)

The x-ray diffraction pattern, Fig. (2a-d), shows (00ℓ) diffraction peaks for both the LCMO and the YBCO layers for bilayer dimensions of d_{LCMO}= 50 nm / d_{YBCO}= 20 nm Fig. (2a), d_{LCMO} = 50 nm / d_{YBCO} = 30 nm Fig. (2b), d_{LCMO} = 50 nm / d_{YBCO}= 50 nm Fig. (2c), and d_{LCMO} = 50 nm / d_{YBCO}= 100 nm Fig. (2d); i.e. they are at least c-axis textured. Furthermore, the sequence of the layers has been changed. YBCO was first grown as bottom layer (here the YBCO structure is controlled by STO substrate) and the LCMO is grown on top. For these samples the same results are found.

In transmission electron microscopy (TEM) images collected at similar samples just consisting of more than two layers[10] (prepared under the same conditions in the identical set-up) it can be found that these samples show atomic flat interfaces. That means, that LCMO and YBCO grow cube on cube by forming structurally a high–quality interface. Consequently we assume that possible perturbations created due to structural variations at the interface can be neglected.



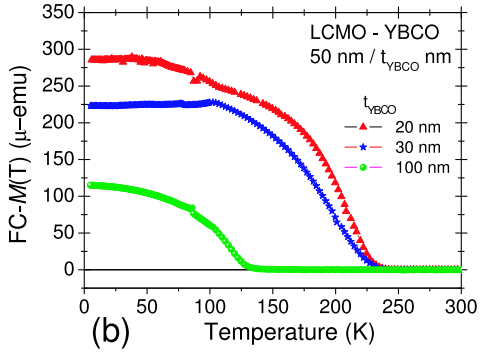


FIG. 3. (Color online) Temperature dependence of the magnetization M(T) after zero–field cooling (a) and field–cooling (b) in an in–plane magnetic field $H_{\rm ext}$ = 10 Oe. Shown are the results for bilayers of $d_{\rm LCMO}$ = 50 nm and $d_{\rm YBCO}$= 20 nm, 30 nm, and 100 nm. The 50 nm / 30 nm bilayer shows two ferromagnetic transitions in the zero–field–cooled measurement (a). The first at $T_{\rm Curie}$ = 229 K can not be seen in the figure the second one occurs at $T_{\rm Curie}$ =180 K. We attribute this behavior to a nonhomogeneous magnetic layer in that sample.

B. Magnetization measurements

Fig. (3a) shows the magnetization M(T) as a function of temperature for three different bilayers. The measurements are performed after zero–field cooling to T = 5 K. Then, the magnetization is measured with increasing temperature in an in-plane external magnetic field of $H_{\rm ext}$ = 10 Oe. The three curves refer to three different bilayers with dimensions of $d_{\rm LCMO}$ = 50 nm and $d_{\rm YBCO}$ = 20, 30, and 100 nm, respectively. In Fig. (3a) starting at low temperatures, we see a negative magnetization that refers to the diamagnetic signal of the dominant superconducting state. With increasing the temperature the magnetization jumps to positive values. This temperature identifies the superconducting transition temperature $T_{\rm c}$. Above the critical temperature $T_{\rm c}$, which depends on the thickness of the YBCO layer, we find a positive magnetization that is caused by the ferromagnetic ordering in the LCMO layer. With increasing temperature the magnetization drops to zero. This temperature identifies the ferromagnetic transition temperature $T_{\rm Curie}$. To prove that the ferromagnetic ordering is also present below the superconducting transition, where the signal is governed by the diamagnetic response of the YBCO layer, also the field-cooled magnetization is measured. The results are given in Fig. (3b). It shows the magnetization M(T) as function of the temperatures for the three different bilayers. The field-cooled measurement M(T) is done in an in-plane external magnetic field of $H_{\rm ext}$ = 10 Oe. Here, two important features are found, first, ferromagnetism occurs in the whole temperature range; $T \leq T_{\rm Curie}$. Second, the ferromagnetic ordering shifts to lower temperatures with increasing thickness of the YBCO layer.

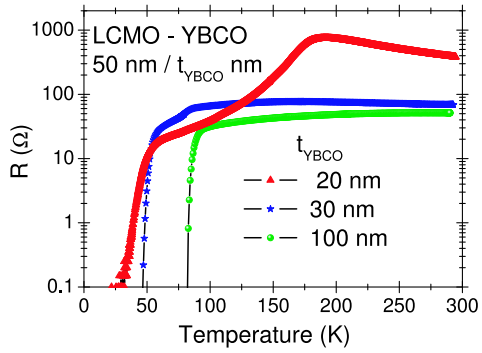


FIG. 4. (Color online) Temperature dependent in-plane resistance R(T) for the same samples as in Fig (3a). The data are collected from standard four-probe measurements.

In addition to the magnetization data we performed electric transport measurements R(T) for the bilayers, as shown in Fig. (4). Three results are given for $d_{\rm LCMO}$ = 50 nm and $d_{\rm YBCO}$= 20 nm, 30 nm, and 100 nm. In case of the thinnest bilayer we find a transition from a semiconductor–like behavior ($dR/dT < 0$) to a metallic–like ($dR/dT > 0$) around T = 180 K. This shows that the properties of the YBCO in the bilayer have to be strongly affected due to the presence of the LCMO layer. Otherwise the large difference in resistivity between YBCO [$\rho_{\rm YBCO}$ (T=300 K) $\approx$ 400 $\mu\Omega cm$] and LCMO [$\rho_{\rm LCMO}$ (T=300 K) $\approx$ 100 $m\Omega cm$] would lead to current flow only in the cuprate layer. But this behavior can only be found in case of bilayers with thicknesses of the YBCO layer of $d_{\rm YBCO}$= 30 nm and 100 nm, respectively. The different R(T) behavior of the 50 nm/20 nm bilayer is therefore related to a diffusion of spin–polarized quasiparticles from the LCMO layer into YBCO.

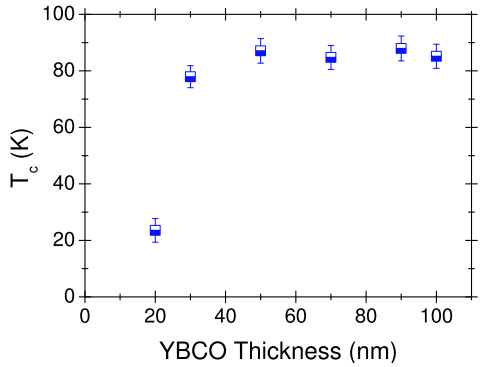


FIG. 5. (Color online) The superconducting transition temperature of bilayers on STO with varying thickness of the YBCO layer obtained from the diamagnetic on–set in the zero–field–cooling magnetization measurements.

From the zero–field cooled magnetization curves M(T) we extract the transition temperature $T_{\rm c}$ of the YBCO film. Here the diamagnetic signal is used to define $T_{\rm c}$, the values are determined by the maximum of the first derivative of M(T). As a result we find a strong decrease

of T_c for bilayers containing thin YBCO layers. In case of 20 nm YBCO film we find T_c= 23 K, for the 30 nm film we find T_c= 76 K, whereas bilayers with thicker YBCO films show transition temperatures between T_c= 85 K and 90 K. A plot of the transition temperatures for different YBCO thicknesses shown in Fig.(5).

Additionally, we want to remark, that not only the transition temperature but also the critical current density in the YBCO layer is affected by the magnetic layer. Magnetic flux pinning inside the superconductor leads to a hysteretic behavior of the critical current density j_c[15,16].

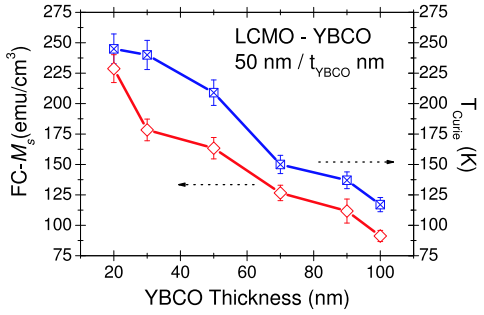


FIG. 6. (Color online) Ferromagnetic ordering temperature $T_{\rm Curie}$ and saturation magnetization M_s of bilayers with varying thickness of the YBCO layer. $T_{\rm Curie}$ is determined from the on–set of the ferromagnetic signal in Fig.(3b). M_s is determined from the saturation signal $M(T)$ in Fig. (3b) divided by the volume of the LCMO layer. $T_{\rm Curie}$ and $M_{\rm s}$ strongly decrease with increasing YBCO thickness.

Another interesting observation in the field–cooled magnetization M(T) in Fig. (3b) is the increase of the ferromagnetic transition temperature with decreasing thickness of the YBCO layer. We measure, for a fixed CMR layer thickness of 50 nm, ferromagnetic transition temperatures $T_{\rm Curie}$ = 245 K, 240 K, and 117 K for the YBCO thicknesses of 20, 30, and 100 nm, respectively. In Fig. (6) a plot of the ferromagnetic ordering temperature $T_{\rm Curie}$ of all bilayer structures as a function of the thickness of the YBCO layer is shown. The 1/3-Ca doped $La_{1-x}Ca_xMnO_3$ compound has a bulk value of $T_{\rm Curie-bulk} \approx 275$ K, for thin films $T_{\rm Curie}$ = 245 K is measured[25]. The reduction of the ferromagnetic ordering temperature may be regarded as indication for a charge transfer from the ferromagnetic layer into the superconductor. However, evidence for this process can not be given from these experiments. We want to address this question by the performance of optical conductivity measurements. These results will be published elsewhere. Concerning the coexistence of the two phenomena (ferromagnetism and superconductivity), we speculate that, the very low in–plane coherence length $\xi_{\rm ab} \approx 1.6$ nm of the high-T_c materials rules out that such a coexistence can be found in more than 1 to 2 unit cells away from the interface.

C. Rough theoretical estimation of $\xi_{\rm FM}$

In this section we present a rough theoretical estimation that is able to describe the observed reduction of the superconducting transition temperature in the investigated bilayer systems. The application of the model allows us finally to give an estimate for the spin diffusion length of the spin polarized quasiparticles from the ferromagnet into the superconductor.

The decay length of the superconducting order parameter $\xi_{\rm prox}$ in the ferromagnetic layer (*proximity effect*) can be written as

$$\xi_{prox} = \frac{\hbar v_F}{\Delta E_{ex}} \qquad (1)$$

where $v_{\rm F}$ is the Fermi velocity and $\Delta E_{\rm ex}$ the exchange splitting energy of the ferromagnetic layer.

So far, oscillations of the superconducting transition temperature T_c in the CMR / d-wave–HTSC superlattices have not been found experimentally[10,13]. This can be understood from the following equation:

$$\xi_{sc} = \sqrt{\frac{\hbar D_{sc}}{k_B T_c}} \qquad (2)$$

where $\xi_{\rm sc}$ is the coherence length; $D_{\rm sc}$ the electron diffusion coefficient in the superconductor; $k_{\rm B}$ is Boltzmann's constant and T_c the critical temperature.

From equations (1) and (2) we conclude that oscillations of the critical temperature T_c of the unconventional superlattices (CMR/d-wave SC) do not occur due to the large exchange energy $\Delta E_{\rm ex} \approx 3$ eV[26] for the hole-doped rare–earth manganites in conjunction with the short coherence length $\xi_{\rm ab} \approx 1.6$ nm, $\xi_c \approx 0.3$ nm for YBCO. Additionally, a very small spin diffusion length $\xi_{\rm FM}$ into the superconducting layer is expected. The nearly full spin polarization (spin↑ or spin↓) at the Fermi level of LCMO leads to quenching not only of the *Andreev reflections*[27] but also of the *proximity effect*, since it prevents the Cooper–pairs to tunnel into the magnetic layer. This also leads to the absence of oscillations of T_c in these CMR/HTSC superlattices.

The pair breaking in CMR/HTSC due to the injection of quasiparticles (QPI) into the superconducting layer has been taken into account[3,12,13]. This phenomenon has been very early investigated by Parker[28] and can be written as:

$$\frac{\Delta(n_{qp})}{\Delta(0)} \approx 1 - \frac{2n_{qp}}{4N(0)\Delta(0)} \qquad (3)$$

where $\Delta(n_{\rm qp})$ is the energy required to suppress the order parameter of the superconductor due to the density of spin polarized quasiparticles $n_{\rm qp}$. N(0) and $\Delta(0)$ give the density of states and the order parameter at $T = 0$ K, respectively. $n_{\rm qp}$ is generated by self-injection along the c-axis across the highly transparent interface and is governed by the high exchange splitting energy $\Delta E_{\rm ex} \approx 3$ eV

of the magnetic layer, see equation (1). The QPI is a temperature dependent function and can be derived in the following form[22,29]:

$$n_{qp}(T) \approx 4N(0)\Delta(0)\sqrt{\frac{\pi}{2}\frac{\Delta(T)k_BT}{\Delta^2(0)}}\ e^{\frac{-\Delta(T)}{k_BT}} \qquad (4)$$

The spin diffusion length $\xi_{\rm FM}$ can now be determined after Ref.[3] analogous to a classical FM/SC structure as:

$$\xi_{FM} \approx \sqrt{\ell_o v_F \tau_s} \qquad (5)$$

Here ℓ_o(T = 0 K) ≈ 20 nm is the mean free path in YBCO[12], the spin diffusion relaxation time τ_s is given by:

$$\tau_s \approx 3.7\frac{\hbar k_B T_c}{\Delta E_{ex}\Delta(T)} \qquad (6)$$

where:

$$\Delta(T) \sim \Delta(0)\sqrt{1-(\frac{T}{T_c})} \qquad (7)$$

with $\Delta(0)$ ≈ 20 meV for YBCO[12]. From equation (3), we end up with a relation where the temperature dependence and the length scale of the spin diffusion length $\xi_{\rm FM}$ is included.

First, we have to consider the spin density in the superconductor. It is assumed that spins in high–temperature superconductors can be described as unitary scatterers. From Zn doping in YBCO it is known that a critical doping in the range of 2-10 % strongly reduces T_c[30–32]. This critical density of spins is achieved at a distance of $d = \alpha\ \xi_{\rm FM}$, with α ≈ 3. This d is now identified with the YBCO film thickness. This enables us to model the experimental data by:

$$d = \alpha\xi_{FM} \cong 3.7\frac{\alpha m^*\hbar v_F^2}{\Delta(0)\Delta E_{ex} n_{qp}(0)e^2}\frac{\sqrt{T/n_{qp}(T)}}{\sqrt[4]{1-(T/T_c)}} \qquad (8)$$

m^* and e are the electron effective mass and charge.

Introducing now $n_{\rm qp}$(T) from equation (4) we are able to fit our experimental data using the quasiparticle density as the only free parameter. This parameter $n_{\rm qp}$(T) describes the decrease of the energy gap $\Delta(n_{\rm qp})$[28,33]. In our case we find the best fitting for $n_{\rm qp}$(T)≈ 0.36, 0.35, and 0.13 for T/T_c = 0.01, 0.3, and 0.9, respectively, which agrees with other theoretical calculations of $n_{\rm qp}$(T)≈ 0.32, 0.31, and 0.09 at the same temperature ratio for d-wave superconductors[29,34]. Figure (7) shows the experimentally determined transition temperatures normalized to the $T_{\rm c-bulk}$=91 K for different film thicknesses on two different substrates $SrTiO_3$ (STO) and $LaSrGaO_4$ (LSGO) and the fit to the rough theoretical estimation.

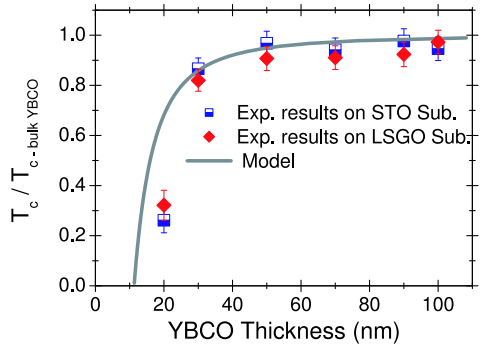


FIG. 7. (Color online) The normalized superconducting transition temperature of bilayers with varying thickness of the YBCO layer on STO and LSGO substrates obtained from the diamagnetic on–set in the zero–field–cooling magnetization measurement (squares) and model according to equation (8) (solid line). The model gives a good description of the experimental data.

The description fits nicely to the experimental results and suggests that the recovery of the transition temperature T_c of the YBCO top layer takes place at about 30 nm which leads to a spin diffusion length of $\xi_{FM} = d/\alpha$ ≈10 nm. This finding is in good agreement with results that have been estimated by Holden et al.[14] from optically investigated LCMO/YBCO superlattices by spectroscopic ellipsometry measurements of the far–infrared (FIR) dielectric properties. These results provide an evidence that the free carrier response is strongly suppressed in these superlattices as compared to pure YBCO and LCMO films, and they estimate that a critical thickness for the YBCO is in the range of 20 nm. Note, that in case of superlattices the spin diffusion quasiparticles penetrate from both sides into to the superconducting film. The accordance between the results shown in this paper and other groups using different experimental techniques gives rise to a spin diffusion length $\xi_{\rm FM}$ from LCMO into YBCO in the order of 10 nm at low temperatures.

IV. CONCLUSION

We have investigated experimentally and estimated theoretically the effects of the diffusion of spin polarized quasiparticles in bilayer structures of manganites and cuprates. From x-ray measurements we have shown that $YBa_2Cu_3O_{7-\delta}$ thin films can be grown epitaxially on thin epitaxial films of $La_{2/3}Ca_{1/3}MnO_3$. Transport and magnetization measurements show the coexistence of ferromagnetism and superconductivity at low temperatures in these structures. We find that the transition temperature of the superconducting film drastically decreases with thinner $YBa_2Cu_3O_{7-\delta}$ films. The development of a simple model allows us to explain the experimental data and enables us to determine the spin diffusion length of spin polarized quasiparticles from $La_{2/3}Ca_{1/3}MnO_3$ into

$YBa_2Cu_3O_{7-\delta}$ to be in the range of $\xi_{FM} \approx 10$ nm.

ACKNOWLEDGMENTS

The authors are grateful to G. Cristiani for the preparation of the outstanding samples, and E. Brücher for SQUID measurements. S.S. is grateful to Max–Planck–Society and Ministry of Higher Education and Scientific Research, Egyptian government for support.

[1] V.L. Ginzburg, Sov. Phys. JETP **4**, 153 (1957).
[2] P.M. Tedrow and R. Meservey, Phys. Rev. Lett. **26**, 192 (1971).
[3] K.E. Gray, in "Nonequilibrium Superconductivity, Phonons and Kapitza Boundaries" , edited by K. E. Gray (Plenum, New York, 1981).
[4] A.I. Buzdin and M. Y. Kupriyanov, JETP Letters **52**, 487 (1990).
[5] Z. Radovic, M. Ledvij, L. Dobrosavljevic, A.I. Buzdin, and J.R. Clem, Phys. Rev. B **44**, 759 (1991), and references therein.
[6] H.K. Wong, B. Y. Jin, H.Q. Yang, J.B. Ketterson, and J.E. Hilliard, J. Low Temp. Phys. **63**, 307 (1986).
[7] J.S. Jiang, D. Davidovic, D.H. Reich, and C.L. Chien, Phys. Rev. Lett.**74**, 314 (1995), and Rev. B **54**, 6119 (1996).
[8] Yu. N. Proshin and M.G. Khusainov, JETP **86**, 930 (1998)
[9] Yu.A. Izyumov, Yu.N. Proshin, and M.G. Khusainov, Phys. Usp. **45**, 109 (2002), and references therein.
[10] H.-U. Habermeier, G. Cristiani, R.K. Kremer, O. Lebedev, G. Van Tendeloo, Physica C **364**, 298 (2001).
[11] A.M. Goldman, V.A. Vas'ko, P.A. Kraus, K.R. Nikolaev, and V.A. Larkin, J. Magn. Magn. Mater. **200**, 69 (1999).
[12] N.C. Yeh, R.P. Vasquez, C.C. Fu, A.V. Samoilov, Y. Li, and K. Vakili, Phys. Rev. B **60**, 10522 (1999).
[13] Z. Sefrioui, D. Arias, V. Pena, J.E. Villegas, M. Varela, P. Prieto, C. Leon, J.L. Martinez, and J. Santamaria, Phys. Rev. B **67**, 214511 (2003).
[14] T. Holden, H.-U. Habermeier, G. Cristiani, A. Golnik, A. Boris, A. Pimenov, J. Humlíček, O. Lebedev, G. Van Tendeloo, B. Keimer, and C. Bernhard, Phys. Rev. B **69**, 064505 (2004).
[15] J. Albrecht, S. Soltan, and H.-U. Habermeier, EuroPhys. Lett. **63**, 881 (2003).
[16] H.-U. Habermeier, J. Albrecht, and S. Soltan, Supercond. Sci. Technol. **17**, S140 (2004).
[17] F. Chen, B. Gorshunov, G. Cristiani, H.-U. Habermeier, and M. Dressel, Solid State Commun. **131**, 295 (2004).
[18] R.J. Soulen, J.M. Byers, M.S. Osofsky, B. Nadgorny, T. Ambrose, S.F. Cheng, P. R. Broussard, C.T. Tanaka, J. Nowak, J.S. Moodera, A. Barry, and J.M.D. Coey, Science **282**, 85 (1998).
[19] M.S. Osofsky, R.J. Soulen, B.E. Nadgorny, G. Trotter, P.R. Broussard, and W.J. Desisto, Mater. Sci. Eng. B **84**, 49 (2001).
[20] M.S. Osofsky, B. Nadgorny, R.J. Soulen, P. Broussard, and M. Rubinstein, J. Byers, G. Laprade, Y.M. Mukovskii, D. Shulyatev, and A. Arsenov, J. Appl. Phys. **85**, 5567 (1999).
[21] J.Y. Wei, J. Superconduct. **15**, 67 (2002).
[22] Y. Gim, A. W. Kleinsasser, and J. B. Barner, J. Appl. Phys. **90**, 4063 (2001).
[23] W.H. Tang, C.Y. Ng, C.Y. Yau, and J. Gao, Supercond. Sci. Technol. **13**, 580 (2000).
[24] J.M. Triscone, Ø. Fischer, O. Brunner, L. Antognazza, A.D. Kent, and M.G. Karkut, Phys. Rev. Lett. **64**, 804 (1990).
[25] R.B. Praus, G.M. Gross, F.S. Razavi, and H.-U. Habermeier, J. Magn. Magn. Mater. **211**, 41 (2000).
[26] M. Quijada, J. Cerne, J.R. Simposon, H.D. Drew, K-H. Ahn, A.J. Millis, R. Shreekala, R. Ramesh, M. Rajeswari, and T. Venkatesan, Phys. Rev. B **58**, 16093 (1998).
[27] A.F. Andreev and Zh. Eksp, Sov. Phys. JETP **19**, 1228 (1964).
[28] W.H. Parker, Phys. Rev. B **12**, 3667 (1975).
[29] E.J. Nicol and J.P. Carbotte, Phys. Rev. B **67**, 214506 (2003).
[30] P.J. Hirschfeld and N.D. Goldenfeld, Phys. Rev. B **48**, 4219 (1993).
[31] M. Franz, C. Kallin, A.J. Berlinsky, and M.I. Salkola, Phys. Rev. B **56**, 7882 (1997).
[32] C.Y. Yang, A.R. Moodenbaugh, Y.L. Wang, Youwen Xu, S.M. Heald, D.O. Welch, M. Suenaga, D.A. Fischer, and J.E. PennerHahn, Phys. Rev. B **42**, 2231 (1990).
[33] C.S. Owen and D.J. Scalapino, Phys. Rev. Lett. **28**, 1559 (1972).
[34] D. Koller, M.S. Osofsky, D.B. Chrisey, J.S. Horwitz, R.J. Soulen, R.M. Stroud, C.R. Eddy, J. Kim, R.C.Y. Auyeung, J.M. Byers, B.F. Woodfield, G.M. Daly, T.W. Clinton, and M. Johnson, J. Appl. Phys. **83**, 6774 (1998).